

# Theoretical description of the total $\gamma^*\gamma^*$ cross-section and its confrontation with the LEP data on doubly tagged $e^+e^-$ events

J. KWIECIŃSKI<sup>a</sup>, L. MOTYKA<sup>b,c</sup>

<sup>a</sup>*Department of Theoretical Physics,*

*H. Niewodniczański Institute of Nuclear Physics, Cracow, Poland*

<sup>b</sup>*High Energy Physics, Uppsala University, Uppsala, Sweden*

<sup>c</sup>*Institute of Physics, Jagellonian University, Cracow, Poland*

## Abstract

We perform a detailed analysis of the total inelastic cross-section for  $\gamma^*\gamma^*$  collisions. Different contributions coming from the quark box diagram, reggeons, the soft and hard pomeron are included. The QCD pomeron contribution contains a dominant part of subleading effects which reduces its intercept and delays the onset of the asymptotic pomeron to high energies. Estimates of the cross-section for doubly-tagged  $e^+e^- \rightarrow e^+e^- \text{hadrons}$  events are presented and compared with the existing LEP data. Good agreement between the theoretical results and the experimental data is found. We also comment on the extraction of the BFKL pomeron intercept from the available LEP measurements.

# 1 Introduction

The study of high energy limit of perturbative QCD is very interesting both theoretically and phenomenologically. The leading asymptotic behaviour of (semi)hard processes is described by the perturbative pomeron which is generated by the ladder diagrams with the reggeised gluon exchange along the chain. The summation is carried out by the celebrated Balitskij-Fadin-Kuraev-Lipatov equation [1, 2]. Although the basic structure of the BFKL pomeron is fairly well understood there are still some theoretical problems which have to be treated with care and are not entirely solved as yet. Thus the QCD pomeron is known to acquire important subleading corrections [3, 4]. In particular the recently computed NLL corrections to the BFKL pomeron intercept are found to dominate over the leading result already at small values of the strong coupling constant  $\alpha_s \sim 0.1$  that invalidates the perturbative expansion for this quantity. Thus the resummation of the perturbative series is necessary in order to cure this problem [5, 6, 7, 8]. Two related approximate approaches have proved to be particularly useful for this purpose: imposing the so-called consistency constraint [7], which follows from the requirement of restricting the gluon kinematics to the quasi-multiregge limit and the other proposed in [6] which combines the leading and subleading BFKL effects with the renormalisation group constraints. Another problem is related to the fact that in the BFKL gluonic ladders the gluon virtualities are not restricted to the hard domain even if the ladder is coupled to hard objects. This is caused by the diffusion of the gluon transverse momenta towards the infrared region which is in fact enhanced when the running of the coupling constant in the BFKL kernel is taken into account [9]. However, it was shown [10] that the BFKL amplitude can be still factorized into the hard and soft part(s).

One of the most promising measurements which can probe the BFKL pomeron is the determination of the total cross-section for hadronic production in the interaction of two virtual photons at high energies [11, 12, 13, 14, 15, 16, 17, 18]. If the virtualities of the photons are large and comparable, the process is fully perturbative and moreover pure LO DGLAP evolution effects are suppressed due to short evolution length, leaving a room for the genuine BFKL contribution to the cross-section. These conditions seem to be realized in the experiments measuring the cross-section for doubly tagged  $e^+e^-$  events at LEP1 and LEP2 [19, 20]. The main purpose of our paper is to analyze the available LEP data in respect to the information about the hard pomeron that it contains. This of course requires detailed treatment of other competing mechanisms, like the quark box diagram contribution, the exchange of the soft pomeron and of the reggeons. Similar analysis has been performed in Ref. [13] where the hard pomeron term was treated phenomenologi-

cally. The novel feature of our approach is the fact that the BFKL pomeron contribution is estimated directly from the exact (numerical) solution of the BFKL equation with the subleading effects generated by the consistency constraint taken into account. In this way we do not restrict ourselves to the asymptotic form of the hard QCD pomeron contribution to the  $\gamma^*\gamma^*$  cross-section. It has been shown in Ref. [18] that this asymptotic form is expected to be delayed to high energies. It is therefore mandatory in the phenomenological analysis of experimental data to disentangle the threshold effects from asymptotic power-like increase of the cross-sections with increasing energy.

The content of our paper is as follows: in the next Section we recall the basic formulas connecting the process  $e^+ e^- \rightarrow e^+ e^- + \text{hadrons}$  with the cross-section for hadron production in  $\gamma^*\gamma^*$  collisions, in Sec. 3 we discuss the “background” to the QCD pomeron contribution to the total  $\gamma^*\gamma^*$  cross-section, i.e. the quark parton model, soft pomeron and reggeon contributions while the QCD pomeron contribution is discussed in Sec. 4. In Sec. 5 we present comparison of our predictions with experimental data from LEP and in Sec. 6 we summarise our results.

## 2 Doubly tagged events

In the equivalent photon approximation the differential cross-section of the process  $e^+e^- \rightarrow e^+e^- + \text{hadrons}$  (averaged over the angle  $\phi$  between the lepton scattering planes in the frame in which the virtual photons are aligned along the  $z$  axis) is given by the following formula [11]:

$$\begin{aligned} \frac{Q_1^2 Q_2^2 d\sigma}{dy_1 dy_2 dQ_1^2 dQ_2^2} &= \left(\frac{\alpha}{2\pi}\right)^2 [P_{\gamma/e^+}^{(T)}(y_1)P_{\gamma/e^-}^{(T)}(y_2)\sigma_{\gamma^*\gamma^*}^{TT}(Q_1^2, Q_2^2, W^2) + \\ &P_{\gamma/e^+}^{(T)}(y_1)P_{\gamma/e^-}^{(L)}(y_2)\sigma_{\gamma^*\gamma^*}^{TL}(Q_1^2, Q_2^2, W^2) + P_{\gamma/e^+}^{(L)}(y_1)P_{\gamma/e^-}^{(T)}(y_2)\sigma_{\gamma^*\gamma^*}^{LT}(Q_1^2, Q_2^2, W^2) + \\ &P_{\gamma/e^+}^{(L)}(y_1)P_{\gamma/e^-}^{(L)}(y_2)\sigma_{\gamma^*\gamma^*}^{LL}(Q_1^2, Q_2^2, W^2)] \end{aligned} \quad (1)$$

where

$$P_{\gamma/e}^{(T)}(y) = \frac{1 + (1 - y)^2}{y} \quad (2)$$

$$P_{\gamma/e}^{(L)}(y) = 2\frac{1 - y}{y} \quad (3)$$

In Eq. (1)  $y_1$  and  $y_2$  are the longitudinal momentum fractions of the parent leptons carried by virtual photons,  $Q_i^2 = -q_i^2$  ( $i = 1, 2$ ) where  $q_{1,2}$  denote the four momenta of the virtual photons and  $W^2$  is the total CM energy squared of the two (virtual) photon system, i.e.

$W^2 = (q_1 + q_2)^2$ . The cross-sections  $\sigma_{\gamma^*\gamma^*}^{ij}(Q_1^2, Q_2^2, W^2)$  are the total cross-sections of the process  $\gamma^*\gamma^* \rightarrow \text{hadrons}$  and the indices  $i, j = T, L$  denote the polarization of the virtual photons. The functions  $P_{\gamma/e}^{(T)}(y)$  and  $P_{\gamma/e}^{(L)}(y)$  are the transverse and longitudinal photon flux factors.

The conditions provided by LEP detectors offer the opportunity to measure both the scattered electrons at the small angle  $\theta$  falling in the range of about 30 to 70 mrad. This corresponds to the virtualities of colliding photons:  $Q_i^2 = 4(1 - y_i)E_{beam}^2 \tan^2(\theta_i/2)$ . Since, typically  $y_i \ll 1$  in such measurements the region of  $Q^2$  equal to a few  $\text{GeV}^2$  is probed at LEP1 and above  $10 \text{ GeV}^2$  at LEP2. Due to rather low statistics for the doubly tagged events one focuses usually on a more inclusive quantity than (1), namely on

$$\frac{d\bar{\sigma}}{dY} = \int dQ_1^2 dQ_2^2 dy_1 dy_2 \frac{d\sigma}{dQ_1^2 dQ_2^2 dy_1 dy_2} C(Q_1^2, Q_2^2, y_1, y_2) \delta\left(Y - \log\left(\frac{y_1 y_2 s}{Q_1 Q_2}\right)\right), \quad (4)$$

where the function  $C(Q_1^2, Q_2^2, y_1, y_2)$  denotes the experimental cuts.

### 3 The background processes

In the high  $Y$  and high  $Q_i^2$  limit the dominant contribution to  $\sigma_{\gamma^*\gamma^*}^{ij}$  comes from the hard pomeron exchange. However for non-asymptotic energies and virtualities the contribution of other mechanisms has to be included. So, when  $Y$  is not large enough the quark box diagram contribution is important for all virtualities. It becomes small for high values of  $W$  decreasing as  $1/W^2$  (modulo logarithmic effects) in this limit. On the other hand, at low  $Q^2$  non-perturbative phenomena i.e. the soft pomeron and for not too large values of  $W$  also the reggeon exchange are important. We shall analyze these components of the cross-section in more detail.

#### 3.1 The quark box contribution

The quark box (or QPM) contribution to the total  $\gamma^*\gamma^*$  cross-sections can at the leading order be calculated exactly and the result is given for instance in Ref. [21]. The impact of the QCD corrections on the result has been shown to be small [22, 23]. There appears some uncertainty due to the choice of the quark masses. To be precise, the quark mass enters the result in two ways – through the virtual quark propagators, where it would be suitable to use the running quark mass at the large scale  $W^2$  and through the wave function and kinematics of the “on-mass-shell” produced quarks, where the pole mass should rather be used. It is not clear how to take into account both requirements simultaneously

so usually one set of masses is used everywhere. The discrepancy for the two possible choices is however small for photons with virtualities above 1 GeV<sup>2</sup>. We have chosen  $m_u = m_d = m_s = 0$  and  $m_c = 1.2$  GeV. The  $b$  quark contribution is negligible due to kinematical effects and the low electric charge.

### 3.2 The soft pomeron

In our approach the soft pomeron represents the contribution to the high energy amplitude coming from the exchange of gluons with their virtualities being in the non-perturbative domain. Since for such configurations the perturbative formalism does not apply we parametrize the corresponding contribution using the Regge model. Thus we employ the Donnachie-Landshoff parameterization of the soft pomeron contribution to the  $\gamma^*(Q^2)p$  cross-section, and using the Gribov factorisation hypothesis we find that the soft pomeron exchange gives the following component of the  $\gamma^*(Q_1^2)\gamma^*(Q_2^2)$  cross-section:

$$\sigma_{\gamma^*\gamma^*}^{SP}(Q_1^2, Q_2^2, W^2) = \frac{\sigma_{\gamma^*p}^{SP}(Q_1^2, W^2)\sigma_{\gamma^*p}^{SP}(Q_2^2, W^2)}{\sigma_{pp}^{SP}(W^2)} \quad (5)$$

where  $\sigma_{\gamma^*p}^{SP}$  and  $\sigma_{pp}^{SP}$  denote the soft pomeron contributions to the  $\gamma^*p$  and  $pp$  total cross-sections respectively. Assuming that the soft pomeron contribution to  $\gamma^*p$  total cross-section should exhibit Bjorken scaling at large  $Q^2$  we find:

$$\sigma_{\gamma^*p}^{SP}(Q^2, W^2) \sim \frac{1}{Q^2} \left( \frac{W^2}{Q^2} \right)^\epsilon \quad (6)$$

where  $\epsilon = \alpha_{SP} - 1$  with  $\alpha_{SP}$  denoting the soft pomeron intercept ( $\alpha_{SP} \approx 1.08$ ). We also have:

$$\sigma_{pp}^{SP}(W^2) \sim \left( \frac{W^2}{W_0^2} \right)^\epsilon \quad (7)$$

with  $W_0 = 1$  GeV. From equations (5, 6) and (7) we get:

$$\sigma_{\gamma^*\gamma^*}^{SP}(Q_1^2, Q_2^2, W^2) \sim \left( \frac{1}{Q_1^2 Q_2^2} \right)^{1+\epsilon/2} \left( \frac{W^2}{Q_1 Q_2} \right)^\epsilon \quad (8)$$

The characteristic feature of the soft pomeron contribution to the total  $\gamma^*\gamma^*$  cross-section is its rapid decrease with increasing virtualities. It follows from equation (8) that for large characteristic scale  $Q^2$  for both photons ( $Q_1^2 \sim Q_2^2 \sim Q^2$ ),  $\sigma^{SP}(Q^2, Q^2, W^2)$  decreases as  $1/Q^{4+2\epsilon} \sim 1/Q^4$  (for fixed  $W^2/Q^2$ ) in contrast to the perturbative QCD pomeron contribution which has only the  $1/Q^2$  behaviour (modulo logarithmic modifications). The soft pomeron contribution should therefore be negligible at large  $Q^2$ .

For the numerical calculations we have used the following Donnachie-Landshoff parameterizations of  $\sigma_{\gamma^*p}^{SP}(Q^2, W^2)$  and  $\sigma_{pp}^{SP}(W^2)$  [26, 27]:

$$\sigma_{\gamma^*p}^{SP}(Q^2, W^2) = \frac{4\pi^2\alpha_{em}}{a_1 + Q^2} A_1 \left( \frac{W^2}{a_1 + Q^2} \right)^\epsilon \quad (9)$$

and

$$\sigma_{pp}^{SP}(W^2) = \sigma_0 \left( \frac{W^2}{W_0^2} \right)^\epsilon \quad (10)$$

where  $A_1 = 0.324$ ,  $a_1 = 0.562 \text{ GeV}^2$ ,  $\epsilon = 0.0808$ ,  $W_0 = 1 \text{ GeV}$ ,  $\sigma_0 = 21.7 \text{ mb}$ .

### 3.3 The reggeons

Exchange of the reggeons (e.g.  $a_0$ ) is another non-perturbative phenomenon which can be described in terms of an isolated Regge pole. The phenomenological analysis of the total hadronic and photoproduction cross-sections (as well as of the  $\gamma^*p$  total cross-section) shows that it is characterized by the Regge intercept close to  $1/2$ , yielding therefore the  $\gamma^*p$  cross-sections behaving approximately like  $1/Q^2(W^2/Q^2)^{-0.5}$ . Its contribution to the  $\gamma^*\gamma^*$  cross-sections may be obtained from the Regge pole contribution to the  $\gamma^*p$ ,  $pp$  and  $p\bar{p}$  cross-sections using the Gribov factorization formula analogous to equation (5). It has to be remembered however that only the  $C$ -even reggeons contribute to the total  $\gamma^*\gamma^*$  cross-section, thus we should average over the reggeon contribution to  $pp$  and  $p\bar{p}$  cross-section in order to find the proton effective coupling to the relevant reggeons. For fixed  $W$ , the reggeon contribution to the  $\gamma^*\gamma^*$  total cross-section has similar dependence on the photon virtuality as the perturbative QCD contribution. The reggeon part of the cross-section decreases with increasing energy approximately like  $1/W$ . We have used the following formula [13] for estimating this component:

$$\sigma_{\gamma^*(Q_1^2)\gamma^*(Q_2^2)}^R = 4\pi^2\alpha_{em}^2 \frac{A_2}{a_2} \left[ \frac{a_2^2}{(a_2 + Q_1^2)(a_2 + Q_2^2)} \right]^{1-\eta} \left( \frac{W^2}{a_2} \right)^{-\eta} \quad (11)$$

with  $A_2 = 0.38$ ,  $a_2 = 0.3 \text{ GeV}^2$  and  $\eta = 0.45$ .

## 4 The QCD pomeron

The hard QCD pomeron is represented by the resummed series of perturbative gluonic ladders which in the leading logarithmic approximation is described by the BFKL equation. In order to take into account (in an approximate way) the non-leading corrections to

the BFKL kernel we use the running coupling constant along the gluonic ladder and the consistency constraint (CC) which follows from the assumption that the virtuality of the gluons exchanged along the ladder is dominated by their transverse momenta squared [7]. The consistency constraint was shown to introduce at the NLL approximation a correction to the pomeron intercept saturating about 70% of the exact NLL result and the collinear limit of the kernel with this constraint is consistent with the requirements of the renormalisation group. At least a part of the remaining correction may be attributed to the running of the coupling constant. Therefore the LO BFKL equation with CC and running coupling constant may be thought of as a simplified model for providing the resummation of leading and subleading BFKL effects. Certainly, the BFKL equation constructed in the framework of perturbative QCD cannot hold when the gluons become too soft. In order to eliminate the contribution from the non-perturbative region we impose a cut-off on the virtualities  $k^2$  of gluons propagating along the ladder:  $k^2 > k_0^2 = 1 \text{ GeV}^2$ . This cut-off reflects the fact that a colour-charge cannot propagate freely in the QCD vacuum and its propagator has a finite correlation length. The contribution from the non-perturbative region is treated phenomenologically, i.e. it is assumed to give the separate soft pomeron component of the cross-section which was discussed in the previous section.

The consistency constraint restricts the available phase-space for the emissions of real gluons — thus suppressing the radiation. The most important consequence is reduction of the pomeron intercept. However it also interlocks the longitudinal and transverse components of the gluon momenta. This makes it possible to define an energy scale for the onset of the Regge regime, since the distribution of the transverse gluon momenta has a natural characteristic scale.

In order to estimate the contribution of the QCD pomeron it is convenient, following our previous treatment in Ref. [18], to introduce the unintegrated gluon distributions  $\Phi_i(k^2, Q^2, x_g)$  in the virtual photon of virtuality  $Q^2$  where  $k^2$  and  $x_g$  denote the gluon transverse momentum squared and the longitudinal momentum fraction of the parent virtual photon carried by the gluon respectively. The index  $i$  corresponds to the transverse or longitudinal polarisation of the virtual photon. The unintegrated gluon distribution  $\Phi_i(k^2, Q^2, x_g)$  satisfies the (modified) BFKL equation which reads:

$$\Phi_i(k^2, Q^2, x_g) = \Phi_i^0(k^2, Q^2, x_g) + \Phi^S(k^2, Q^2, x_g)\delta_{iT} + \frac{3\alpha_s(k^2)}{\pi}k^2 \int_{x_g}^1 \frac{dx'}{x'} \int_{k_0^2}^{\infty} \frac{dk'^2}{k'^2} \left[ \frac{\Phi_i(k'^2, Q^2, x')\Theta\left(k^2 \frac{x'}{x_g} - k'^2\right) - \Phi_i(k^2, Q^2, x')}{|k'^2 - k^2|} + \frac{\Phi_i(k^2, Q^2, x')}{\sqrt{4k'^4 + k^4}} \right] \quad (12)$$

where the function  $\Theta\left(k^2 \frac{x'}{x_g} - k'^2\right)$  reflects the consistency constraint. The inhomogeneous

term  $\Phi_i^0(k^2, Q^2, x_g)$  corresponds to the quark box and crossed box contribution to the un-integrated gluon distribution in the photon and the term  $\Phi^S(k^2, Q^2, x_g)\delta_{iT}$  corresponds to the soft pomeron contribution to this distribution. The detailed definition of those two functions is given in Ref. [18].

The QCD pomeron contribution to the  $\gamma^*\gamma^*$  total cross-sections  $\sigma_{\gamma^*\gamma^*}^{ij}(Q_1^2, Q_2^2, W^2)$  is given by the following formula:

$$\sigma_{\gamma^*\gamma^*}^{ij}(Q_1^2, Q_2^2, W^2) = \frac{1}{2\pi} \sum_q \int_{k_0^2}^{k_{max}^2(Q_2^2, x)} \frac{dk^2}{k^4} \int_{\xi_{min}(k^2, Q_2^2)}^{1/x} d\xi G_q^{0j}(k^2, Q_2^2, \xi) \Phi_i(k^2, Q_1^2, x\xi) \quad (13)$$

where

$$k_{max}^2(Q_2^2, x) = -4m_q^2 + Q_2^2 \left( \frac{1}{x} - 1 \right) \quad (14)$$

$$\xi_{min}(k^2, Q_2^2) = 1 + \frac{k^2 + 4m_q^2}{Q_2^2} \quad (15)$$

and

$$x = \frac{Q_2^2}{2q_1q_2} \quad (16)$$

The impact factors  $G_q^{0j}(k^2, Q_2^2, \xi)$  are defined in Ref. [18]. The increase of the function  $\Phi_i(k^2, Q_1^2, x_g)$  with decreasing  $x_g$  which follows from the BFKL equation, generates increase of the cross-section  $\sigma_{\gamma^*\gamma^*}(Q_1^2, Q_2^2, W^2)$  with increasing  $W^2$ . This is implied by the fact that  $x_g \sim x$  (cf. Eq. (13)).

Let us recall that in the conventional leading  $\log(1/x)$  approximation we should set  $\Phi_i^0(k^2, Q^2, x_g = 0)$  in place of  $\Phi_i^0(k^2, Q^2, x_g)$  in the BFKL equation (12). It is also legitimate in this approximation to set just  $x$  instead of  $x\xi$  as the argument of  $\Phi_i$  in equation (13) and neglect all phase space limitations constraining integrations over  $d\xi$  and  $dk^2$ . These approximations lead to the following approximate expression for the  $\gamma^*\gamma^*$  cross-sections:

$$\sigma_{\gamma^*\gamma^*}^{ij}(Q_1^2, Q_2^2, W^2) = \frac{1}{2\pi} \sum_q \int_{k_0^2}^{\infty} \frac{dk^2}{k^4} \Phi_i^0(k^2, Q^2, x_g = 0) \bar{\Phi}_i(k^2, Q_1^2, x) \quad (17)$$

where the function  $\bar{\Phi}_i(k^2, Q_1^2, x)$  corresponds to the solution of the BFKL equation with the inhomogeneous term equal to  $\Phi_i^0(k^2, Q^2, x_g = 0)$  instead of  $\Phi_i^0(k^2, Q^2, x_g)$ . It should be emphasised that formula (13), which our estimate of the QCD pomeron contribution is based upon contains important kinematical effects which are missing in its approximate asymptotic form (17). First of all equation (13) includes the phase space effects generated by the kinematical limits constraining integrations over  $d\xi$  and  $dk^2$ . Moreover we do



also keep  $x_g$  dependence in the impact factors  $\Phi_i^0(k^2, Q^2, x_g)$  defining the inhomogeneous term of the BFKL equation. The variable  $x_g$  is limited from below by  $x$ . It provides a kinematical lower bound for the longitudinal momentum fraction  $z_q$  of the quark emitting the gluon in the quark box diagram defining the impact factors  $\Phi_i^0(k^2, Q^2, x_g)$ , i.e.  $z_q > x_g > x$  [18]. By keeping the  $x_g$  dependence of the impact factors  $\Phi_i^0(k^2, Q^2, x_g)$  we generate corrections to their asymptotic form in the limit  $x_g \rightarrow 0$  which are subleading (have an additional factor of  $x_g$ ) but non-negligible even for low values of  $x_g$ .

These effects, i.e. the phase-space limitations in equation (13) and the  $x_g$  dependence of the impact factors  $\Phi_i^0(k^2, Q^2, x_g)$  delay the onset of the asymptotic (power-like) behavior of the total cross-sections. They also introduce an additional energy dependence of the cross-sections in the low  $W$  region which is essentially of kinematical origin. In particular, they are entirely responsible for generating sub-asymptotic energy dependence of the Born term (i.e. given by the two gluon exchange) which in the high energy limit gives the constant cross-section (see Fig. 1). Finally, it is worthwhile to note that such threshold effects may be misidentified as the asymptotic, power-like rise of the cross-section giving too high value of the pomeron intercept.

It follows from our previous analysis [18] of the QCD pomeron contribution to  $\gamma^*\gamma^*$  total cross-section(s) that the resulting pomeron intercept equals about 0.35 whereas the asymptotic, power-like behaviour is reached roughly when  $W^2 > 20 Q_1 Q_2$  (see Fig.1). In terms of the commonly used variable  $Y$  this means that we should expect the power-like rise of the cross-section to start only at  $Y > 3$  and giving a substantial effect for  $Y > 5$ . Such effect seems to appear in the recent L3 data [19].

The definition of the impact factors is straightforward in the leading order approximation of perturbative QCD in which they are given by the quark box diagrams contribution. In this approximation the impact factors are proportional to  $\Phi_i^0(k^2, Q^2, x_g = 0)$ . However the leading order expressions may be affected by the possibly important subleading corrections which are not known yet <sup>1, 2</sup>. Thus the non-leading corrections introduce some uncertainty into our result. Besides that the value of the scale for the running strong coupling constant describing the interaction between quarks and gluons is ambiguous. In fact both these problems are related and an improvement here can only be achieved when the non-leading corrections to the impact-factors become known. A natural choice for the scale  $\mu^2$  of the running coupling constant  $\alpha_s(\mu^2)$  would be the virtuality of the inter-

---

<sup>1</sup>In our framework we take into account a part of the subleading corrections which are of the kinematical origin.

<sup>2</sup>The calculation of the NLO corrections to the impact factors is in progress [28].

acting gluon  $k^2$  ( $k^2 > 0$ ), possibly combined with the relevant quark mass  $m_q$  squared:  $\mu^2 = k^2 + m_q^2$ . However, because there is some freedom left here one may use also an alternative choice of  $\mu^2$ , e.g.  $\mu^2 = (k^2 + m_q^2)/4$  in order to check the uncertainty of the prediction and possibly find an experimental hint on the proper choice of the scale. These uncertainties do only affect normalisation of the cross-sections leaving unchanged their energy dependence. We have confronted the predictions obtained with the use of both scenarios with the experimental data from LEP. The lower scale scenario yields the  $\gamma^*\gamma^*$  cross-section two times bigger than that obtained with the standard choice of  $\mu^2 = k^2 + m_q^2$  but still slightly below the data. Thus it is clear that at present the LEP data favour taking the low scale in the impact factors. Of course this conclusion may be altered if the NLO corrections to impact factors turn out to be positive and large.

## 5 Comparison with the data

### 5.1 Do we see the pomeron?

L3 and OPAL collaborations have collected a sample of data for double tagged events both at the  $Z^0$  peak and for the  $e^+e^-$  between 183 and 202 GeV [19, 20]. In Fig. 2 and Fig. 3 we give the comparison between the theoretical results obtained in the framework of our model and the data. Our theoretical predictions include all components of the  $\gamma^*\gamma^*$  cross-section discussed in previous sections and are obtained using formula (4) with L3 and OPAL cuts and binning respectively. It can be seen that the model reproduces the experimental results rather well although we tend to overestimate the L3 data from LEP1 and underestimate those from LEP2. We point out that the hard pomeron dominates the cross-section for  $Y > 3.5 - 4$  so this region of  $Y$  is particularly interesting. Moreover, in the LEP1 data the non-perturbative contributions coming from the soft pomeron and the reggeons are still of considerable importance whereas at LEP2 energies they become of little relevance. This is fortunate because these non-perturbatively driven components of the cross-section are known with a rather limited accuracy due to errors of fits and some theoretical ambiguities (in particular the interplay between the soft and hard pomeron). On the other hand the quark-box contribution is known very accurately so the uncertainty which is introduced when subtracting this component from the total cross-section is small. Therefore the LEP2 data, especially those for  $Y > 3.5 - 4$  carry the most precise information about the QCD pomeron. It is also in the large  $Y$  region where we expect the significant BFKL enhancement of the cross-section.

Let us also quote comparisons between the data and the PHOJET Monte-Carlo pro-

gram [24] presented by L3 and OPAL. PHOJET contains all the components of the  $\gamma^*\gamma^*$  cross-section but the “hard pomeron” part is described there in the framework of DGLAP evolution only while the BFKL-type effects are neglected. Since the virtualities of both photons are comparable this essentially corresponds to the two gluon exchange process. Therefore, if our conclusions are correct, it should work rather well up to  $Y = 4$ . Indeed it does but already for  $4 < Y < 6$  (at  $\sqrt{s} = 183$  GeV) the data published by both the LEP experiments are slightly underestimated and for the L3 measurement at  $5 < Y < 7$  (at  $\sqrt{s} > 189$  GeV) the PHOJET prediction of  $d\sigma/dY = 30$  fb is below the data ( $d\sigma/dY_{exp} = 80 \pm 10 \pm 10$  fb) by more than three standard deviations. Our result in this bin reads 52 fb being by two standard deviations below the preliminary experimental point. However (see Fig. 2) we describe rather well the energy dependence of the pomeron contribution, perhaps underestimating the overall normalisation of this term. The OPAL data have larger error bars and cover a smaller region of  $Y$  than the L3 data. So, the tendency reported by OPAL that  $d\sigma/dY(Y)$ , estimated with the PHOJET MC, underestimates the central values of the experimental points at high  $Y$  is not yet statistically significant. However, our model reproduces the OPAL data better, i.e. has lower  $\chi^2$ , than PHOJET. The data from both the experiments confirm also our prediction that the onset of the power-like increase of the  $\gamma^*\gamma^*$  cross-section is delayed to  $Y > 3.5$ .

Let us finally point out the problem with radiative QED corrections to the double tagged cross-section. It has been noticed in Ref. [20], that if the  $\gamma^*\gamma^*$  collision energy  $W$  is obtained directly from a measurement of the kinematics of tagged electrons, as done by L3, the estimated and actual value of  $W$  may be different. This discrepancy is mainly caused by the electromagnetic initial state radiation since the emitted ISR photons which have small enough virtuality are not seen by the detector. Nevertheless they can carry a non-negligible fraction of the lepton energy, affecting therefore the determination of  $W$  based on the measurement of leptonic four-momenta. This effect is suppressed by a small factor  $\alpha_{em}/\pi$  but after performing an integration over the photon virtuality giving a large logarithm, it appears to be sizable [20]. According to our knowledge the L3 collaboration has not included this important correction in the analysis. This means that the L3 data, especially for large  $Y$  may change, namely  $d\sigma/dY$  may turn out to be smaller. The OPAL collaboration uses produced hadronic invariant mass to calculate  $W$  and thus the OPAL data are not affected by such a systematic error. The consistency between our predictions and the OPAL data is very good.

## 5.2 On the determination of the intercept

One of the important aims of the empirical analysis of experimental data on the reaction  $e^+e^- \rightarrow e^+e^- + \text{hadrons}$  with tagged leptons is the determination of the effective QCD pomeron intercept which describes the high  $W$  behaviour of the  $\gamma^*\gamma^*$  cross-section. In order to extract directly this cross-section from the experimental results with doubly tagged events it is necessary to perform a deconvolution using photon luminosity functions. Furthermore, one has to subtract the remaining components of the cross-section. Then the results are usually given as a function  $d\sigma_{\gamma^*\gamma^*}/dY$  of the variable  $Y$  and the asymptotic form of the BFKL cross-section

$$\frac{d\sigma_{\gamma^*\gamma^*}}{dY} \sim \frac{1}{Q_1 Q_2} \frac{\exp[(\alpha_P - 1)Y]}{\sqrt{Y}} \quad (18)$$

is fitted with the pomeron intercept  $\alpha_P$  being left as a free parameter.

We would however like to point out that this method of determining the pomeron intercept may not be correct. We understand that in the fitting procedure it is usually assumed that the  $Q_i^2$  distributions are the same in each of the  $Y$ -bins and do not affect the fits of  $Y$  dependence. However, the variable  $Y$  is in fact correlated with  $Q_1 Q_2$  and we may expect the distribution of  $Q_1 Q_2$  to be dominated by the low photon virtualities for high  $Y$  bins and by the high values of the virtualities for low  $Y$ . In this case we would obtain some enhancement of the effective  $\gamma^*\gamma^*$  cross-section for high  $Y$  due to strong  $1/(Q_1 Q_2)$  dependence of the total cross-section. This effect may imitate the genuine increase of total cross-sections with increasing  $W^2$ . In Fig. 4 we show that such effect indeed occurs. In this figure we plot the effective cross-sections  $\bar{\sigma}_{\gamma^*\gamma^*}^{TT}(Y)$  (for the L3 cuts) obtained with different assumptions concerning  $\sigma_{\gamma^*\gamma^*}^{TT}(W^2, Q_1^2, Q_2^2)$ . We used the following definition of  $\bar{\sigma}_{\gamma^*\gamma^*}^{TT}(Y)$  (cf. formula (4)):

$$\bar{\sigma}_{\gamma^*\gamma^*}^{TT}(Y) = \frac{\int dQ_1^2 dQ_2^2 dy_1 dy_2 U(y_1, y_2, Q_1^2, Q_2^2; Y) \sigma_{\gamma^*\gamma^*}^{TT}(W^2, Q_1^2, Q_2^2)}{\int dQ_1^2 dQ_2^2 dy_1 dy_2 U(y_1, y_2, Q_1^2, Q_2^2; Y)} \quad (19)$$

where the weight factor  $U$  reads

$$U(y_1, y_2, Q_1^2, Q_2^2; Y) = C(Q_1^2, Q_2^2, y_1, y_2) \frac{P_{\gamma/e}^{(T)}(y_1)}{Q_1^2} \frac{P_{\gamma/e}^{(T)}(y_2)}{Q_2^2} \delta\left(Y - \log\left(\frac{y_1 y_2 s}{Q_1 Q_2}\right)\right). \quad (20)$$

The effective  $\gamma^*\gamma^*$  cross-section defined in this way should directly correspond to the experimental measurements of  $\sigma_{\gamma^*\gamma^*}^{TT}(Y)$ .

The modification of the  $Y$  dependence can be seen at best when looking on the dashed curves which correspond to the asymptotic two-gluon contribution which gives completely flat  $W$  dependence. The different magnitude of photon virtualities in different  $Y$ -bins

generates the effective intercept  $\bar{\alpha}_P \sim 1.1$  at LEP1 conditions and  $\bar{\alpha}_P \sim 1.05$  at LEP2. So, the conclusions based on the simple fits to  $\bar{\sigma}_{\gamma^*\gamma^*}(Y)$  would lead to overestimate of the intercept, whose true value was  $\alpha_P = 1$ . This is not a dramatic effect but still goes beyond the claimed accuracy of the determination of the intercept. A simple remedy to remove such problems would be to use in the fit the quantity  $\langle Q_1 Q_2 \rangle(Y) \bar{\sigma}_{\gamma^*\gamma^*}(Y)$  for the pomeron mediated part of the total  $\sigma_{\gamma^*\gamma^*}(Y)$ , instead of  $\bar{\sigma}_{\gamma^*\gamma^*}(Y)$ . The factor  $\langle Q_1 Q_2 \rangle(Y)$  stands for the mean values of  $Q_1 Q_2$  in the given  $Y$  bin. Then the sensitivity to the virtualities should become substantially reduced.

## 6 Summary and conclusions

In this paper we have performed a theoretical analysis of the  $\gamma^*\gamma^*$  total cross-section assuming the QCD pomeron exchange together with the contributions given by the soft pomeron, the non-pomeron reggeons and by the QPM term. The QCD pomeron contribution was calculated from the numerical solution of the modified BFKL equation in which we have included the dominant subleading effects generated by the consistency constraint limiting the available phase space (see Eq. (12)). We have also included phase space effects in the corresponding formula which connects the total  $\gamma^*\gamma^*$  cross-section(s) with the solution of the BFKL equation (see Eq. (13)). These effects delay the onset of the asymptotic QCD pomeron contribution. The soft pomeron and non-pomeron reggeon terms were estimated using Gribov factorisation. Our theoretical predictions have been obtained with only one adjustable parameter characterizing the energy scale  $\mu^2$  for the running coupling constant in the impact factors and were found to give a reasonable description of the experimental data from LEP. We have found that the soft pomeron and reggeon contributions are important at LEP1. They are however less significant at LEP2 over the entire  $Y$  range. This is linked with the fact that the magnitudes of the virtualities  $Q_{1,2}^2$  which are sampled at LEP2 are larger than those at LEP1. The QPM contribution is very important for low values of  $Y$ . The region of large values of  $Y$  is dominated by the QCD pomeron contribution. To summarise we have found that although the QCD pomeron exchange mechanism is important for the description of the LEP data the other contributions, i.e. QPM and the soft pomeron and non-pomeron reggeons are non-negligible and should be included in the analysis. The QCD pomeron should however give the dominant contribution at energies which will be probed in future linear  $e^+e^-$  colliders.

## Acknowledgments

We are indebted to Gunnar Ingelmann for critically reading the manuscript and valuable comments. We thank Sandy Donnachie, Mariusz Przybycień and Albert De Roeck for very useful and inspiring discussions. LM is grateful to the Swedish Natural Science Research Council for the postdoctoral fellowship. This research was partially supported by the EU Fourth Framework Programme ‘Training and Mobility of Researchers’, Network ‘Quantum Chromodynamics and the Deep Structure of Elementary Particles’, contract FMRX-CT98-0194 and by the Polish Committee for Scientific Research (KBN) grant NO 2P03B 05119.

## References

- [1] E.A. Kuraev, L.N. Lipatov and V.S. Fadin, Zh. Eksp. Teor. Fiz. **72** (1977) 373 (Sov. Phys. JETP **45** (1977) 199); Ya. Ya. Balitzkij and L.N. Lipatov, Yad. Fiz. **28** (1978) 1597 (Sov. J. Nucl. Phys. **28** (1978) 822); J.B. Bronzan and R.L. Sugar, Phys. Rev. **D17** (1978) 585; T. Jaroszewicz, Acta. Phys. Polon. **B11** (1980) 965; L.N. Lipatov, in “Perturbative QCD”, edited by A.H. Mueller, (World Scientific, Singapore, 1989), p. 441.
- [2] L.N. Gribov, E.M. Levin and M.G. Ryskin, Phys. Rep. **100** (1983) 1.
- [3] V.S. Fadin, L.N. Lipatov, Nucl. Phys. **B477** (1996) 767; Phys. Lett. **B429** (1998) 127; V.S. Fadin, M.I. Kotskii, R. Fiore, Phys. Lett. **B359** (1995) 181; V.S. Fadin, M.I. Kotskii, L.N. Lipatov, hep-ph/9704267; V.S. Fadin, R. Fiore, A. Flachi, M. Kotsky, Phys. Lett. **B422** (1998) 287;
- [4] M. Ciafaloni, G. Camici, Phys. Lett. **B386** (1996) 341; *ibid.* **B412** (1997) 396; Erratum – *ibid.* **B417** (1998) 390; Phys. Lett. **B430** (1998) 349-354; J.R. Forshaw, G.P. Salam, R.S. Thorne, J. Phys. **G25** (1999) 1495-1500; G.P. Salam, Acta Phys. Polon. **B30** (1999) 3679.
- [5] D.A. Ross, Phys. Lett. **B431** (1998) 161; G.P. Salam, JHEP **9807** (1998), 19; M. Ciafaloni, D. Colferai; Phys. Lett. **B452** (1999) 372; S.J. Brodsky et al., JETP Lett. **70** (1999) 155; C.R. Schmidt, hep-ph/9904368.
- [6] M. Ciafaloni, D. Colferai, G.P. Salam, Phys. Rev. **D60** (1999) 114036; JHEP **9910** (1999) 017.

- [7] B. Andersson, G. Gustafson, H. Kharraziha, J. Samuelsson, Z. Phys. **C71** (1996) 613; J. Kwieciński, A.D. Martin, P.J. Sutton, Z. Phys. **C71** (1996) 585.
- [8] J.Kwieciński, A.D. Martin and A.M. Staśto, Phys. Rev. **D56** (1997) 3991.
- [9] B. Andersson, G. Gustafson, H. Kharraziha, Phys. Rev. **D57** (1998) 5543.
- [10] J. Collins and J. Kwieciński, Nucl. Phys. **B316** (1989) 307; M. Ciafaloni, D. Colferai, G. P. Salam, JHEP **0007** (2000) 054.
- [11] S.J. Brodsky, F. Hautmann, D.A. Soper, Phys. Rev. **D56** (1997) 6957; Phys. Rev. Lett. **78** (1997) 803 (Erratum-ibid. **79** (1997) 3544).
- [12] J. Bartels, A. De Roeck, H. Lotter, Phys. Lett. **B389** (1996) 742; J. Bartels , A. De Roeck, C. Ewerz, H. Lotter, hep-ph/9710500.
- [13] A. Donnachie, H.G. Dosch and M. Rueter, Eur. Phys. J. **C13** (2000) 141.
- [14] A. Donnachie, S. Söldner-Rembold, hep-ph/0001035.
- [15] N.N. Nikolaev, J. Speth, V.R. Zoller, hep-ph/0001120; E. Gotsman, E. Levin, U. Maor, E. Naftali, Eur. Phys. J. **C14** (2000) 511.
- [16] J. Bartels, C. Ewerz, R. Staritzbichler, hep-ph/0004029.
- [17] V. T. Kim, L. Lipatov, G.B. Pivovarov, hep-ph/9911228.
- [18] J. Kwieciński and L. Motyka, Phys. Lett. **B462** (1999) 203.
- [19] The L3 Collaboration, (M. Acciari et al.), Phys. Lett. **B453** (1999) 94; P. Achard for the L3 Collaboration, Nucl. Phys. Proc. Suppl. **82** (2000) 61; L3 Note 2568 (2000), presented at the XXXth ICHEP, Osaka, Japan, July 2000.
- [20] M. Przybycień for the OPAL Collaboration, talk at the Photon 2000 conference, Ambleside, England, August 2000.
- [21] V.M. Budnev, I.F. Ginzburg, G.V. Meledin and V.G. Serbo Phys. Rept. **15** (1974) 181.
- [22] C. T. Hill and G. G. Ross, Nucl. Phys. **B148** (1979) 373.
- [23] V. Del Duca, talk at the QCDNET 2000 meeting, Paris, France, September 2000.
- [24] R. Engel, J. Ranft, Phys.Rev. **D54** (1996) 4244.

- [25] A. Białas, W. Czyż, W. Florkowski, Eur. Phys. J. **C2** (1998) 683; W. Florkowski, Acta Phys. Polon. **28** (1997) 2673; A. Donnachie, H.G. Dosch, M. Rueter, Phys. Rev. **D59** (1999) 74011; M. Boonekamp et al., Nucl. Phys. **B555** (1999) 540.
- [26] A. Donnachie and P.V. Landshoff, Phys. Lett. **B296** (1992) 227.
- [27] A. Donnachie and P.V. Landshoff, Z. Phys. **C61** (1994) 139.
- [28] J. Bartels, S. Gieseke and C.F. Qiao hep-ph/0009102.



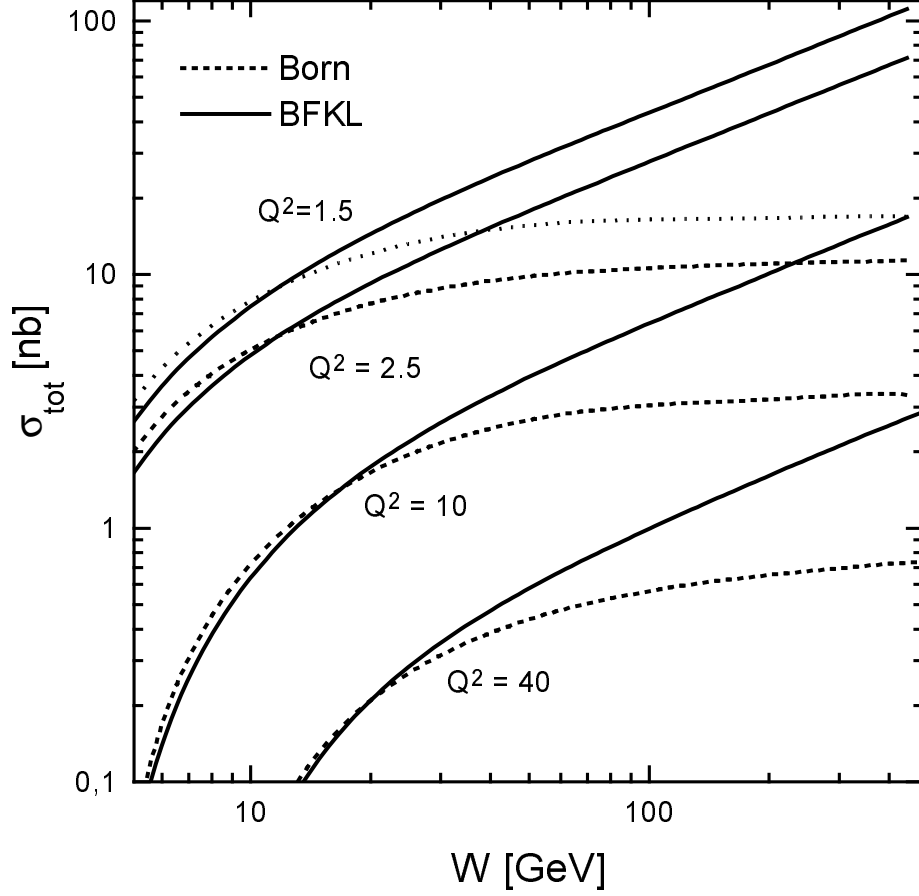


Figure 1: Energy dependence of the cross-section  $\sigma_{\gamma^* \gamma^*}^{TT}(Q_1^2, Q_2^2, W^2)$  for the process  $\gamma^*(Q_1^2) \gamma^*(Q_2^2) \rightarrow \text{hadrons}$  for various choices of photon virtualities  $Q^2 = Q_1^2 = Q_2^2$ : Comparison of the complete contribution of the perturbative QCD pomeron to the cross-section  $\sigma_{\gamma^* \gamma^*}^{TT}(Q^2, Q^2, W^2)$  (continuous line) with its Born term component corresponding to the two gluon exchange mechanism (dotted line). The figure from Ref. [18].

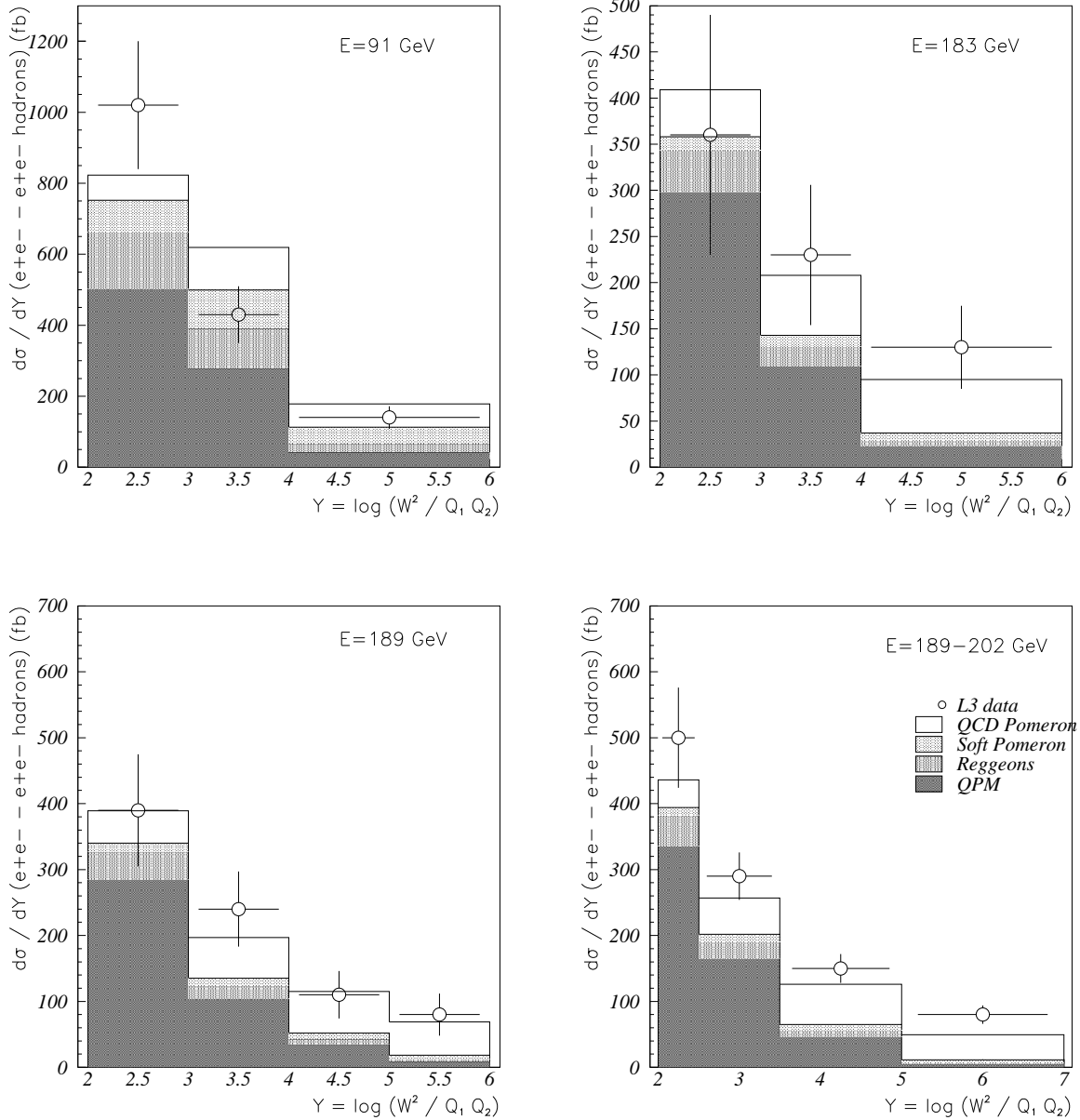


Figure 2: Comparison of the L3 data [19] on the differential cross-section for doubly tagged events  $d\sigma(e^+e^- \rightarrow e^+e^- + \text{hadrons})/dY$  with our predictions plotted as function of  $Y$  for different  $e^+e^-$  collision energies, corresponding to the measurements by the L3 collaboration. Four different mechanisms contributing to  $d\sigma/dY$  are described in the text.

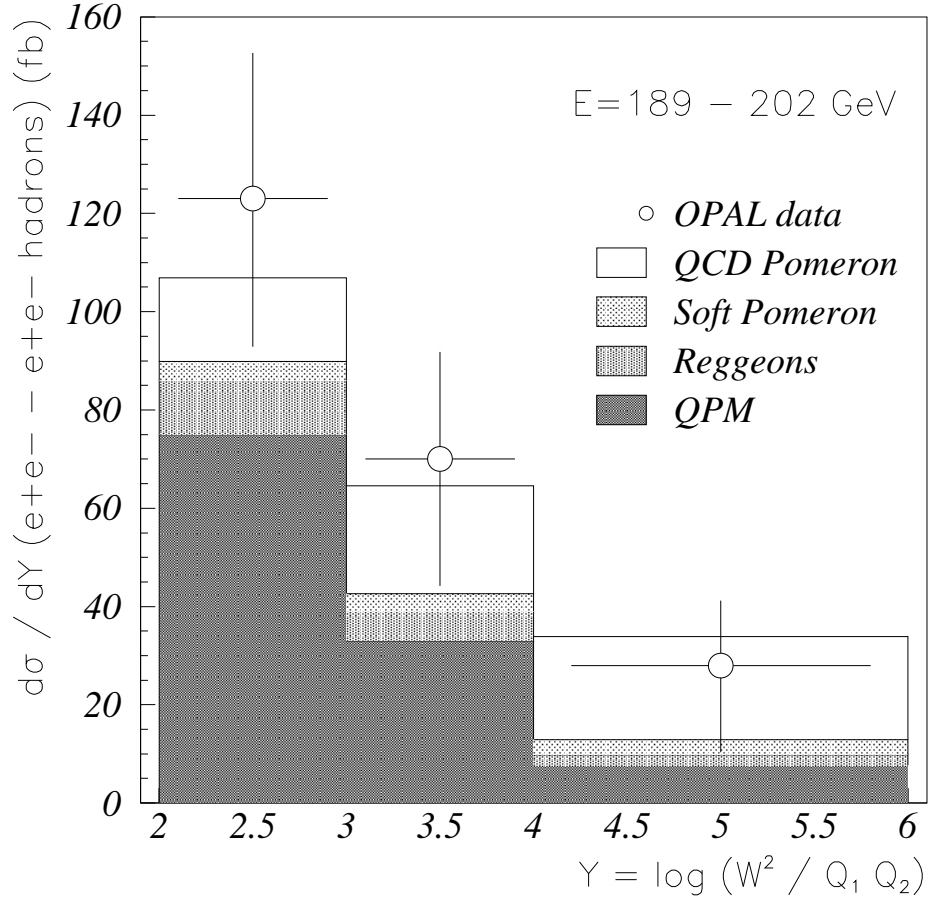


Figure 3: Comparison of the OPAL preliminary data [20] on the differential cross-section for doubly tagged events  $d\sigma(e^+e^- \rightarrow e^+e^- + \text{hadrons})/dY$  with our predictions plotted as function of  $Y$  for the  $e^+e^-$  collision energies between 189 and 202 GeV.

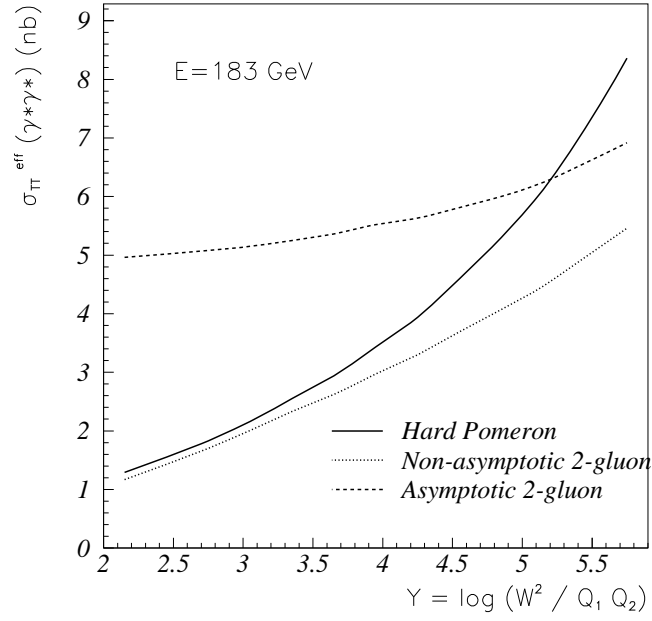
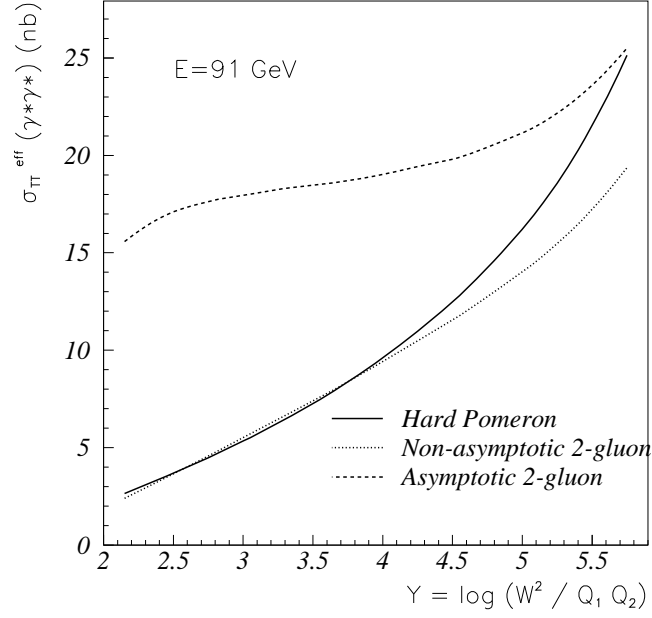


Figure 4: Effective  $\gamma^*\gamma^*$  cross-section defined by formula (19) for transverse photons obtained with L3 cuts for two different  $e^+e^-$  energies. Three curves are shown corresponding to the hard pomeron (continuous line), two gluon exchange (dotted line) and the two gluon exchange in the limit of asymptotically high energies (dashed line) approximations of  $\sigma_{\gamma^*\gamma^*}^{TT}(Q_1^2, Q_2^2, W^2)$ .